In situ detection of single micron-sized magnetic beads using magnetic tunnel junction sensors

Cite as: Appl. Phys. Lett. **86**, 253901 (2005); https://doi.org/10.1063/1.1952582
Submitted: 01 December 2004 • Accepted: 16 May 2005 • Published Online: 16 June 2005

Weifeng Shen, Xiaoyong Liu, Dipanjan Mazumdar, et al.

In situ detection of single micron-sized magnetic beads using magnetic tunnel junction sensors

Weifeng Shen,[a] Xiaoyong Liu,[b] Dipanjan Mazumdar, and Gang Xiao[c]
Physics Department, Brown University, Providence, Rhode Island 02912

(Received 1 December 2004; accepted 16 May 2005; published online 16 June 2005)

We have demonstrated the use of highly sensitive magnetic tunnel junction (MTJ) sensors for the detection of individual micron-sized magnetic labels. By integrating the MTJ sensor into a microfluidic channel, we were able to detect the presence of moving superparamagnetic beads (Dynabeads® M-280) in real time by direct measurement of the magnetic dipole fields associated with single beads. The dipolar fields of a single bead were sufficient to obtain a signal of 80 μV with signal to noise ratio of 24 dB in an applied field of 15 Oe. Our data show conclusively that MTJ sensors are very promising candidates for future applications involving the accurate detection and identification of biomolecules with magnetic labels. © *2005 American Institute of Physics*. [DOI: 10.1063/1.1952582]

In the past decade, significant effort has been put towards the detection of magnetic micro- and nano-particles using spintronic sensors. This work has led to the development of the new spintronic immunoassay (SIA) technology.[1–3] In these magnetic sensor-based biological applications, the detection of the presence or absence of magnetic labels is one of the key issues. On-chip giant magnetoresistive (GMR) sensors have been extensively studied as biosensors for biomolecular detection and recognition.[4–7] However, to the best of our knowledge, no one has yet attempted to apply magnetic tunnel junctions (MTJs) to this emerging SIA application. In this letter, we report our results on detecting superparamagnetic beads in solution using MTJ sensors combined with microfluidic channels.

MTJ devices have been developed for commercial applications in magnetoresistive random access memory[8] and magnetic field sensing.[9] Compared with GMR sensors, MTJs offer higher magnetoresistance (MR) ratios and therefore higher sensitivity at low fields. As a result, MTJs are better suited for the accurate detection of the small (<1 Oe) fields, which are typically encountered in biological applications. In addition, very large magnetoresistances (over 200%) have recently been observed in MTJ devices using MgO tunnel barriers.[10,11] These values are an order of magnitude superior to those reported for contemporary GMR sensors. In addition, MTJ sensors can be integrated into high-density magnetic sensor arrays due to their current-perpendicular-to-plane geometry.[12] These arrays should be capable of on-chip multianalyte detection. In this letter, we demonstrate that a single MTJ sensor has the ability to detect single magnetic beads, with an average signal level of 80 μV and a signal-to-noise ratio (SNR) of 24 dB.

The MTJ sensors used in our study had the following layer structure: Pt (300 Å)/Py (30 Å)/FeMn (130 Å)/Py (60 Å)/Al_2O_3 (7 Å)/Py (120 Å)/Pt (200 Å). Py stands for permalloy. The sensors were patterned using standard optical lithography followed by Ar ion-beam etching; detailed MTJ sensor fabrication processes are described in a previous work.[13,14] We have used elliptical junctions with lateral dimensions of 2×6 μm throughout this work. Figure 1 shows a typical transfer curve of one such MTJ sensor with a MR ratio of 15.3% and a device resistance of 142 Ω. Over the field range of 0–15 Oe, a magnetic sensitivity of 0.4%/G is typical for these sensors.

We have used a microfluidic channel to funnel magnetic beads in solution toward the active area of the MTJ device. SU-8, a negative photoresist, was used to define microchannels as masters on a silicon wafer. Polydimethysiloxane (PDMS) was then poured onto the master and cured for 1 h at 75 °C. The microchannel was replicated into PDMS and mounted directly over the sensor active area. In order to bond the sensor with the PDMS channel, both were treated in oxygen plasma for 1 min and then pressed together.[15,16] Figure 2(a) is an optical image of the finished sensor die after integration with the microfluidic channel. The channel used in our experiment had a height of 50 μm and a width of 600 μm.

Superparamagnetic Dynabeads® (M-280) are polymer beads with an even dispersion of iron oxide (γ-Fe_2O_3) nanoparticles, and are commonly used as magnetic labels for

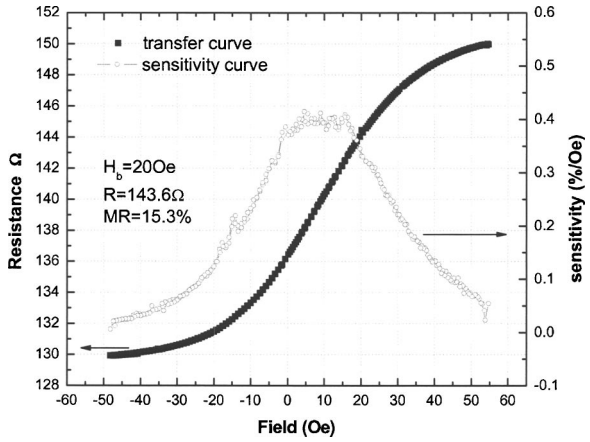

FIG. 1. A typical MTJ transfer curve showing the device resistance of a MTJ sensor in an external applied field. The most sensitive region occurs over the range 0–15 Oe.

[a]Electronic mail: shen@physics.brown.edu
[b]Also at: Micro Magnetics, Inc., 421 Currant Road, Fall River, Massachusetts 02720.
[c]Electronic mail: xiao@physics.brown.edu

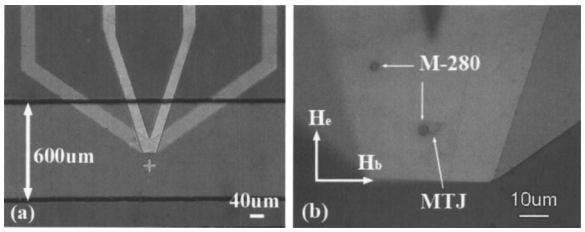

FIG. 2. Optical images of (a) a single 2×6 μm MTJ sensor sealed inside a 600 μm wide microchannel, and (b) an identical sensor with two single M-280 beads in close proximity. The orientation of the two external fields H_e and H_b is also shown in (b).

biomolecules.[4] They have a highly uniform spherical shape with a diameter of 2.8 μm and a susceptibility of $\sim$0.04.[7] Magnetic microbeads (M-280) were dispersed in deionized (DI) water ultrasonically, and then pumped into the microchannel through microtubes. A syringe pump (World Precision Instruments' SP101i) was used to control the rate of fluid flow through the channel, down to a minimum flow rate of 0.01 mL/min. Because M-280 beads have a higher density ($\sim$1.3 g/cm^3) than DI water, the beads will settle at the bottom of the channel at sufficiently slow flow rates. In this case, the beads will roll along the bottom surface of the channel, which is coincident with the top of the MTJ sensor die, ensuring a minimal separation between the beads and the MTJ sensor. Figure 2(b) shows an optical image of a single 2.8 μm diameter bead sitting on the sensor area.

The sensor is operated in an ac bridge configuration and the signal extracted using a lock-in technique. Two crossed pairs of toroidal electromagnets provide in-plane static magnetic fields H_e (in the sensing direction) and H_b (perpendicular to the sensing direction). These applied fields bias the MTJ sensor, allowing it to operate in its most sensitive and linear region (Fig. 1 shows a typical transfer curve). When a bead comes near the MTJ sensor, the magnetic dipole field of the superparamagnetic particle cancels a small fraction of the applied field at the MTJ, resulting in a sensor resistance drop ΔR_{sen} from R^0_{sen} to R_{sen}. The corresponding voltage change across the bridge is given by

$$V_{\mathrm{sig}} = \frac{\tilde{V}_{\mathrm{bias}}}{\sqrt{2}} \frac{(R_2R_3 - R_{\mathrm{sen}}R_4)}{(R_4+R_2)(R_3+R_{\mathrm{sen}})} = \frac{\tilde{V}_{\mathrm{bias}}}{\sqrt{2}R_3} \frac{(R^0_{\mathrm{sen}} - R_{\mathrm{sen}})}{(1+R^0_{\mathrm{sen}}/R_3)(1+R_{\mathrm{sen}}/R_3)}, \quad (1)$$

where $\tilde{V}_{\mathrm{bias}}$ is the ac bias voltage cross the bridge, R_2 (variable), R_3, and R_4 are the resistances of the three arms of the bridge, and R_{sen} is the sensor resistance. Assuming a balanced bridge, $R_2 \approx R^0_{\mathrm{sen}}$, $R_3 = R_4$. When $R_3 \gg R_{\mathrm{sen}}, R^0_{\mathrm{sen}}$, Eq. (1) can be simplified:

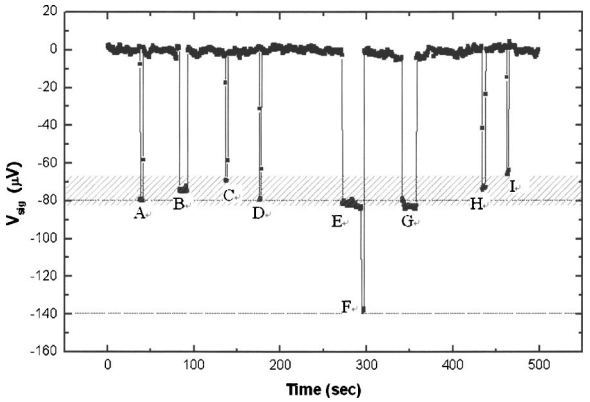

FIG. 3. Real-time voltage data demonstrating single-bead detection. When a single bead passes by the sensor, a sharp signal drop is observed (points A, C, D, H, and I). When a bead becomes stuck on the sensor area for an extended length of time, a plateau signal is obtained (points B and G). Two-step signals (points E and F) correspond to a situation wherein two beads are attached to the junction at the same time. The shadowed band indicates the typical signal range measured for a single bead.

$$V_{\mathrm{sig}} \approx \frac{\tilde{V}_{\mathrm{bias}}}{\sqrt{2}R_3}(R^0_{\mathrm{sen}} - R_{\mathrm{sen}}) = \frac{\tilde{V}_{\mathrm{bias}}}{\sqrt{2}R_3}\Delta R_{\mathrm{sen}}, \quad (2)$$

where ΔR_{sen} is the sensor resistance drop due to the presence of magnetic beads. The ac voltage used to bias the bridge ($\tilde{V}_{\mathrm{bias}}$) was chosen to be 1 V, corresponding to a voltage drop of $\sim$60 mV rms across the MTJ sensor itself. The bias voltage frequency was set to 8 kHz to minimize the effects of $1/f$ noise.

Figure 3 plots the real-time voltage output of the MTJ sensor for an interval during which several beads pass over the MTJ one at a time. Each sharp signal drop (points A, C, D, H, and I) corresponds to an event where a single bead passes by the sensor quickly. Plateaus are observed (points B and G) when the beads stick to the sensor area for a longer interval. Points E and F correspond to a situation where two beads are attached to the junction simultaneously. Starting from point E, a single bead sits on the sensor for about 20 seconds, during which a voltage of $\sim$80 μV is observed. At point F, another bead approaches the sensor and sticks to it along with the first one for about 3 s. This results in an additional contribution to the sensor voltage of $\sim$60 μV (point E).

In Table I, we summarize the parameters used in these measurements. A consistent average signal of 80 μV was observed for single beads over many measurements. This figure corresponds to a SNR of 24 dB, which is superior to that reported for GMR sensors.[6,7] It should be noted that for some beads (points C, H, and I) the signal level is less than 80 μV. This can be explained by a variation in the bead-to-sensor separation for different beads, since the motion of the beads in the microfluidic channel is not well controlled. The observed signal is highest when beads cross over the central

TABLE I. Experimental parameters and average signal-to-noise ratio for single magnetic bead detection, calculated from many measurements.

Sensor size (μm$\times$$\mu$m)	$\tilde{V}_{\mathrm{bias}}$ (V, rms)	$\tilde{V}_{\mathrm{MTJ}}$ (mV, rms)	$R^0_{\mathrm{sen}}(R_{\mathrm{leads}})/R_3$ (Ω)	H_b (Oe)	H_e (Oe)	$V_{\mathrm{sig}}/V_{\mathrm{noise}}$ (μV)	ΔR_{sen} (Ω)
2×6 ellipse	1	60	142(250)/2000	20	15	80/5	0.16Ω

area of the sensor. The amplitude of this signal variation is denoted by the shadowed region in Fig. 3. The size of this area can be considered the normal signal range for a single bead.

The magnetic dipole field generated by a single M-280 bead in the sensing direction in a 15 Oe external field was calculated using finite element simulations (FEMLAB®). The distance between the M-280 bead and the active area of the MTJ is estimated to be 1.8 μm (consisting of the 1.4 μm bead radius, plus a 0.2 μm contact layer, and 0.2 μm of passivation). The bead is assumed to sit at the center of sensor area. Integrating over the full extent of the sensing area, an average field value of 0.4 Oe was obtained, corresponding to a resistance change of 0.22 Ω. This value is consistent with experimental results and indicates that the MTJ sensor is easily capable of detecting suboersted magnetic fields in an aqueous environment. Encouraged by these results, we are currently designing high-density MTJ senor arrays that will be integrated into DNA probes for high-sensitivity DNA fragment detection.

In summary, we have fabricated a series of highly sensitive micron-scale MTJ sensors that have been used to detect the presence of single superparamagnetic M-280 beads. Microfluidic channels were integrated with the MTJ sensors in order to transport M-280 beads in solution to the sensor area. Real-time measurements of the sensor voltage show a series of drops of similar amplitude, where each signal drop corresponds to the passing of a single bead over the MTJ sensor area. The signal amplitude corresponding to a single bead is dependent on the effective bead-to-sensor distance. In general, we have obtained an average signal of 80 μV for a single bead, with a SNR of 24 dB. These results demonstrate the potential for using MTJ sensors for biomolecular detection. In future studies, we intend to fabricate high-density MTJ sensor arrays to improve the performance of the technique.

The authors thank D. Reich, S. Karsk, and A. Hultgren for helpful discussions. This work was supported by DARPA/AFOSR Grant No. F49620-02-1-0307 and by the National Science Foundation Grant Nos. DMR-0306711 and DMR-0080031.

[1]K. Kriz, J. Gehrke, and D. Kriz, Biosens. Bioelectron. **13**, 817 (1998).
[2]J. Richardson, P. Hawkins, and R. Luxton, Biosens. Bioelectron. **16**, 989 (2001).
[3]D. L. Graham, H. A. Ferreira, and P. P. Freitas, Trends Biotechnol. **22**, 455 (2004).
[4]D. R. Baselt, G. U. Lee, M. Natesan, S. W. Metzger, P. E. Sheehan, and R. J. Colton, Biosens. Bioelectron. **13**, 731 (1998).
[5]M. M. Miller, P. E. Sheehan, R. L. Edelstein, C. R. Tamanaha, L. Zhong, S. Bounnak, L. J. Whitman, and R. J. Colton, J. Magn. Magn. Mater. **225**, 138 (2001).
[6]D. L. Graham, H. Ferreira, J. Bernardo, P. P. Freitas, and J. M. S. Cabral, J. Appl. Phys. **91**, 7786 (2002).
[7]G. Li, V. Joshi, R. L. White, S. X. Wang, J. T. Kemp, C. Webb, R. W. Davis, and S. Sun, J. Appl. Phys. **93**, 7557 (2003).
[8]S. Tehrani, J. M. Slaughter, M. Deherrera, B. N. Engel, N. D. Rizzo, J. Salter, M. Durlam, R. W. Dave, J. Janesky, B. Butcher, K. Smith, and G. Grynkewich, Proc. IEEE **91**, 703 (2003).
[9]D. Lacour, H. Jaffrès, F. Nguyen Van Dau, F. Petroff, A. Vaurès, and J. Humbert, J. Appl. Phys. **91**, 4655 (2002).
[10]S. Yuasa, T. Nagahama, A. Fukushima, Y. Suzuki, and K. Ando, Nat. Mater. **3**, 868 (2004).
[11]S. S. P. Parkin, C. Kaiser, A. Panchula, P. M. Rice, B. Hughes, M. Samant, and S.-H. Yang, Nat. Mater. **3**, 862 (2004).
[12]J. S. Moodera, L. R. Kinder, T. M. Wong, and R. Meservey, Phys. Rev. Lett. **74**, 3273 (1995).
[13]X. Y. Liu, C. Ren, and G. Xiao, J. Appl. Phys. **92**, 4722 (2002).
[14]X. Y. Liu, C. Ren, L. Ritchie, B. D. Schrag, G. Xiao, and L. F. Li, J. Magn. Magn. Mater. **267**, 133 (2003).
[15]D. C. Duffy, J. C. McDonald, O. J. A. Schueller, and G. M. Whitesides, Anal. Chem. **70**, 4974 (1998).
[16]T. Deng, H. Wu, S. T. Brittain, and G. M. Whitesides, Anal. Chem. **72**, 3176 (2000).